Solar Energy Materials & Solar Cells 132 (2015) 80–85

Contents lists available at ScienceDirect

Solar Energy Materials & Solar Cells

journal homepage: www.elsevier.com/locate/solmat

Nano-sized indium-free MTO/Ag/MTO transparent conducting electrode prepared by RF sputtering at room temperature for organic photovoltaic cells

Chung-Hyeon Lee [a,b,1], Rina Pandey [a,d,1], Byung-Yong Wang [a,c], Won-Kook Choi [a,d], Duck-Kyun Choi [b], Young-Jei Oh [a,d,*]

[a] Future Convergence Research Division, Korea Institute of Science and Technology (KIST), Hwarangno 14-gil 5, Seongbuk-gu, Seoul 136-791, South Korea
[b] Department of Materials Science and Engineering, Hanyang University, Haengdang 1-dong, Seongdong-gu, Seoul 133-791, South Korea
[c] Department of Materials Science and Engineering, Korea University, Anam-dong 5-1, Seongbuk-gu, Seoul 136-701, South Korea
[d] Department of Nano materials Science and Engineering, Korea University of Science and Technology (KUST), Gajeong-ro 217, Yuseong-gu, Daejeon 305-350, South Korea

ARTICLE INFO

Article history:
Received 19 April 2014
Received in revised form
9 August 2014
Accepted 22 August 2014

Keywords:
Mn doped tin oxide (MTO)
MTO/Ag/MTO multilayer
Sheet resistance
Transmittance
Conventional bulk hetero-junction organic photovoltaic cells

ABSTRACT

As an alternative to indium–tin oxide (ITO), MTO/Ag/MTO (MAM) multilayer transparent electrodes with a nano-sized Ag thin film embedded between Mn-doped tin oxide (MTO) layers were prepared. The MTO/Ag/MTO thin films were deposited on a glass substrate by RF sputtering at room temperature to evaluate their characteristics as transparent electrodes for organic photovoltaic cells (OPVs). Optical and electrical properties of the single layer MTO were investigated at various working pressures and oxygen partial pressures. Based on the optimal condition, the MTO/Ag/MTO multilayer electrode showed a sheet resistance of 10.1–10.6 Ω/sq and transmittance of 80.1–85.4% in the visible range (λ=380–780 nm). Their values are compatible with commercial indium–tin oxide (ITO). Conventional-type bulk hetero-junction organic photovoltaic cells (BHJ-OPVs) using the MTO/Ag/MTO multilayer electrode show an open circuit voltage (V_{OC}) of 0.62 V, a short circuit current (J_{SC}) of 7.12 mA/cm^2, a fill factor (FF) of 0.62, and a power conversion efficiency (PCE) of 2.73%. This PCE is comparable with a commercial ITO electrode (3.17%). This suggests that the MTO/Ag/MTO multilayer electrode is a new promising transparent conducting electrode for BHJ-OPVs.

1. Introduction

The transparent conductive oxide (TCO) thin film is a necessary element for photo electronic devices as an electrode in the area of organic light-emitting diodes (OLEDs) and organic photovoltaic cells (OPVs) [1–3]. The organic photovoltaic cell (OPV) has several merits such as lowcost, renewability and energy harvest due to a simple structure and easy manufacturing process [4–7]. For high power conversion efficiency (PCE), the OPV requires a high-transmittance and low-sheet resistance. Indium–tin oxide (ITO) thin film is very widely used for various photo electronics as transparent electrode due to outstanding optical and electrical properties [8]. However, the indium resource is limited and the production cost of ITO is high due to its manufacturing process which requires high-temperature and high-pressure. Moreover, it is also difficult to apply into a flexible device because it is non-flexible [9–11]. Therefore, it is necessary to develop TCO material manufactured with low-cost and low-temperature, which is comparable to those of ITO. To overcome these problems, oxide/metal/oxide (OMO) structures as a transparent conducting electrode were reported. Recently, ZTO/Ag/ZTO, AZO/Ag/AZO, GZO/Ag/GZO, ZnO/Ag/ZnO and SnO_X/Ag/SnO_X multilayer electrodes have been investigated for indium-free TCOs for OPVs [12–15]. In this work, we studied a new Mn-doped tin oxide (MTO) thin film. In general tin oxide is highly acid resistant, air-stable, low-cost, has good transparency, and can exist at room temperature in the amorphous crystalline phase, which indicates that the surface is very smooth and thus very useful for the formation of multilayer structures. However, there have been a few reports on the optical and electrical properties of Mn-doped SnO_2 thin film until now due to the complexity of the valence state of Mn ion [15–16]. It is expected that Mn ions inclined to incorporate into the lattice in

* Corresponding author at: Future Convergence Research Division, Korea Institute of Science and Technology (KIST), Hwarangno 14-gil 5, Seongbuk-gu, Seoul 136-791, South Korea.
E-mail address: youngjei@kist.re.kr (Y.-J. Oh).
[1] These authors contributed equally to this work.

http://dx.doi.org/10.1016/j.solmat.2014.08.025
0927-0248/

the form of Mn^{3+} (65 pm) ions or Mn^{4+} (54 pm) since their ionic radius is smaller than that of Sn^{4+} (69 pm) [16]. Moreover optical, electrical, and dilute magnetic properties of Mn-doped SnO_2 will be interesting as multiple valence of Mn–SnO_2 thin films varies. Furthermore, recently we reported that bulk Mn-doped SnO_2 showed an electrical p-type conversion by the increase of relative Mn^{3+} valence and was investigated by lower valence cations as acceptor [17], which increases the hole concentration. Even though, the MTO single layer as the anode electrode is difficult to apply to OPVs due to limited optical and electrical properties compared to ITO, there is no report on multilayer transparent electrodes using manganese doped tin oxide (MTO). The MTO/Ag/MTO (MAM) multilayer electrode is studied as the anode electrode with conventional type OPVs, which has high transmittance, low sheet resistance and possibility of deposition at room temperature. Conventional BHJ-OPVs using the MTO/Ag/MTO multilayer transparent electrode and commercial ITO electrode are compared.

2. Experimental details

The MTO/Ag/MTO multilayer electrode was deposited on a patterned glass substrate at room temperature by RF sputtering. The patterned glass substrate was prepared by a photo mask for the OPV electrode. The MTO bottom layer was deposited on the glass substrate with optimized growth conditions at a base pressure of 1×10^{-6} Torr, working pressure of 5.0 mTorr, rf sputter power of 100 W and oxygen partial pressure of 1% at room temperature. After deposition of the MTO bottom layer, the Ag layer was deposited at the base pressure of 2.0×10^{-7} Torr, working pressure of 2.1 mTorr, and rf sputter power of 58 W at room temperature. Finally, the MTO top layer was deposited under the same conditions as the MTO bottom layer. Optical and electrical properties of the MTO/Ag/MTO multilayer electrode were observed by a UV–vis spectrophotometer (Perkin Elmer UV/Vis spectrometer Lambda 18) within the wavelength range of 200–900 nm and hall measurements (Ecopia HMS 3000). X-ray diffraction (XRD) analysis (Rigaku Dmax 2500/server) with CuKα radiation (wavelength (λ) =1.5418 Å) was performed to investigate the crystallographic structure of single (MTO) and multilayer (MAM) thin films. A cross-sectional microstructure of the fabricated MTO/Ag/MTO multilayer electrode was measured by a transmission electron microscope (Taitan TEM). Work function of the optimized MTO/Ag/MTO multilayer electrode was measured by an ultraviolet photo-electron spectroscope (UPS Phi 5000 Versaprobe). Surface morphology of the Ag thin film on the MTO bottom layer was observed by a scanning electron microscope (NOVA Nano SEM 200). Bulk hetero junction OPVs (BHJ-OPVs) were fabricated by the optimized MTO/Ag/MTO multilayer electrode and the commercial ITO (JMC, Korea) electrode under the same condition. They were cleaned for 10 min using acetone, ethanol, and deionized water. PEDOT:PSS (Heraeus)/methanol (Aldrich) (1:1 wt %) solution for a hole transfer layer (HTL) was mixed for 24 h in a glove box and then spin-coated at 4000 rpm for 40 s on the MTO/Ag/MTO transparent electrode. The specimen was annealed at 130 °C for 30 min on the hot-plate in a glove box. As the next step, solutions of P3HT (Rieke Metals, Inc.) of 18 mg and PCBM (Nano caters) of 10.8 mg in 1 ml of chlorobenzene were mixed for 24 h as a photoactive layer and then spun-coated on the hole transfer layer at 2500 rpm for 40 s, and then was annealed at 150 °C for 10 min in a glove box. Finally, LiF and Al electrodes were deposited by a vacuum evaporator with the thickness of 0.6 nm and 100 nm, respectively. The schematic diagram of the conventional BHJ-OPVs structure using the MTO/Ag/MTO multilayer electrode is shown in Fig. 1.

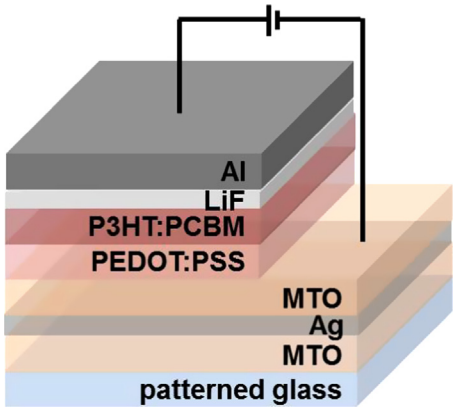

Fig. 1. Schematic diagram of conventional BHJ-OPVs having MTO/Ag/MTO multilayer electrode.

3. Results and discussion

3.1. Single MTO and Ag thin film

Transmittance and sheet resistance of the deposited MTO single layer at room temperature as a function of working pressure and oxygen partial pressure are shown in Fig. 2(a) and (b). With increasing working pressure from 2.0 to 5.0 mTorr, sheet resistance decreased down to 35 kΩ/sq and transmittance increased from 70.2% to 74.5% as shown in Fig. 2(a). In Fig. 2(b), transmittance was increased from 68.1% to 84.3% as the oxygen partial pressure (0–4%) was increased while the sheet resistance was

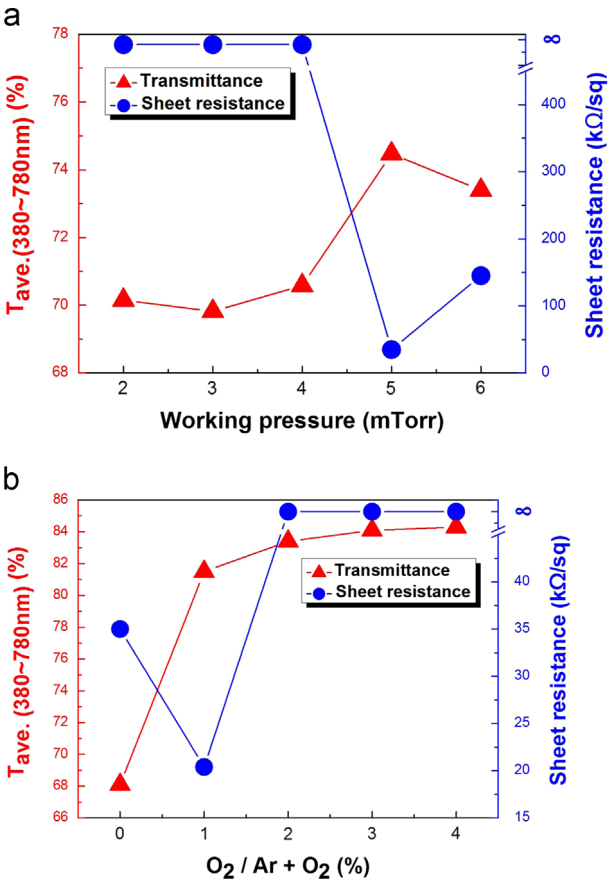

Fig. 2. Average transmittance and sheet resistance of MTO thin film as a function of (a) working pressure and (b) oxygen partial pressure.

decreased from 35 to 20.4 kΩ/sq at 1% ($O_2/Ar+O_2$). In this study, a sheet resistance of 20.4 kΩ/sq and transmittance of 81.5% were obtained at the oxygen partial pressure of 1% ($O_2/Ar+O_2$). The XRD spectra of the Mn-doped tin oxide (MTO) thin films with different oxygen partial pressures (0–5.0 at.%) are plotted in the 2θ ranges 20–80°. All the as-deposited MTO films grown at room temperature are found to be of amorphous structure (see Fig. S1, Supporting information). The electrical properties of binary layer Ag/MTO/glass are shown in Fig. 3(a). When the Ag thickness is increased, resistivity decreases because of increase of both electron mobility and carrier concentration. Fig. 3(b) shows the surface morphology of Ag thin film deposited on the MTO bottom layer as a function of thickness. A smooth surface was observed at the Ag thicknesses of 9 and 10 nm. As the figure has shown, islands seemed to play a role of interrupting the electron movement as a resistance, which deteriorated electronic property. However, a dense surface was observed at 11 and 12 nm Ag thicknesses. When the thickness of the Ag film was increased, it filled the voids between the islands. As a consequence, carrier concentration and electron mobility were increased. Fig. 3(c) shows the figure of merit (F_{TC}) at a wavelength of 550 nm when a Ag thin film was deposited on the MTO bottom layer. As a result, the best value at the thickness of 11 nm for Ag thin film was a transmittance of 75.2% and sheet resistance of 10 Ω/sq. Therefore, the thickness of the Ag thin film was optimized at 11 nm. F_{TC} was calculated by Eq. (1), as defined by Haacke [18], where T is transmittance at the wavelength of 550 nm, and R_S is sheet resistance. This equation is commonly adopted for evaluation of the transparent electrode:

$$F_{TC} = \frac{T^{10}}{R_S} \quad (1)$$

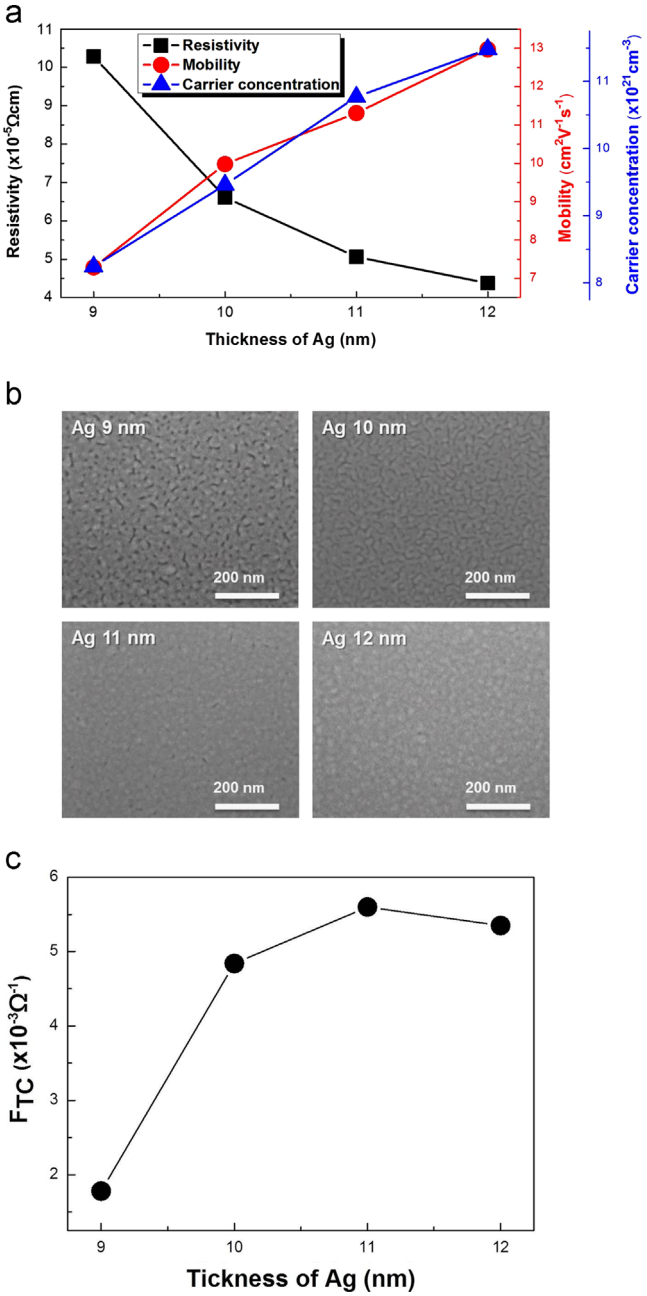

Fig. 3. (a) Electrical properties, (b) SEM surface image and (c) figure of merit (F_{TC}) of Ag/MTO/Glass binary layer with various thickness of Ag thin film.

3.2. MTO/Ag/MTO multilayer electrode

The MTO thin films with the variations of thickness (30–45 nm) were used as the top and bottom layers. Ag thin film was deposited on the MTO bottom layer with the thickness of 11 nm, as explained in Fig. 3(c). The transmittance of the MTO/Ag/MTO multilayer electrode as a function of thickness of the MTO thin films and commercial ITO (as comparison) are shown in Fig. 4. As shown in Table 1, T_{ave} (380–780 nm) and sheet resistance of the MTO/Ag/MTO multilayer electrode are 85.4% and 10.1 Ω/sq at the thickness of 40 nm MTO thin film respectively. These results are comparable with the commercial ITO, which shows a transmittance of 86.61% and sheet resistance of 12.23 Ω/sq. In addition, F_{TC} has a better performance of $2.85 \times 10^{-2}\,\Omega^{-1}$ when compared to the commercial ITO ($2.59 \times 10^{-2}\,\Omega^{-1}$). Sheet resistance ($R_s$) of the MTO/Ag/MTO multilayer electrode was calculated by Eq. (2) using Ohm's law [19]. Fig. 5 shows the cross-sectional image of the

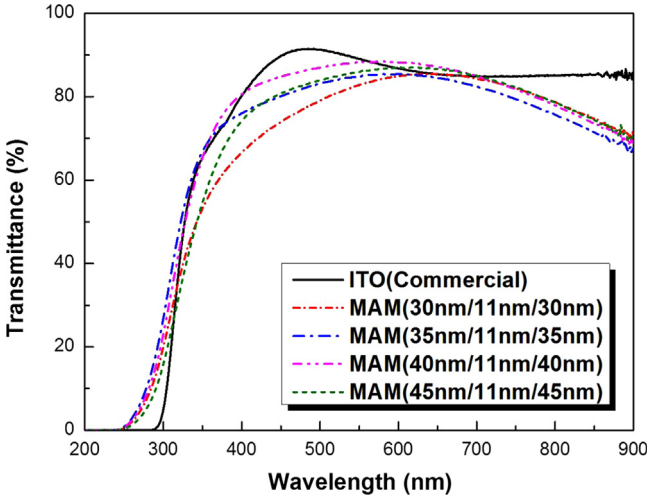

Fig. 4. Transmittance of MTO/Ag/MTO multilayer electrode as a function of thickness of MTO thin film and commercial ITO.

Table 1
Comparison of transmittance, sheet resistance and F_{TC}.

Transparent electrode	T_{ave} (380–780 nm) (%)	T_{at} 550 nm (%)	R_S (Ω/sq)	F_{TC} ($\times 10^{-2}\Omega^{-1}$)
ITO (Commercial)	86.6	89.1	12.2	2.59
MAM (30/11/30)	80.1	82.7	10.4	1.45
MAM (35/11/35)	82.1	84.8	10.6	1.81
MAM (40/11/40)	85.4	88.1	10.1	2.85
MAM (45/11/45)	83.2	85.8	10.3	2.12

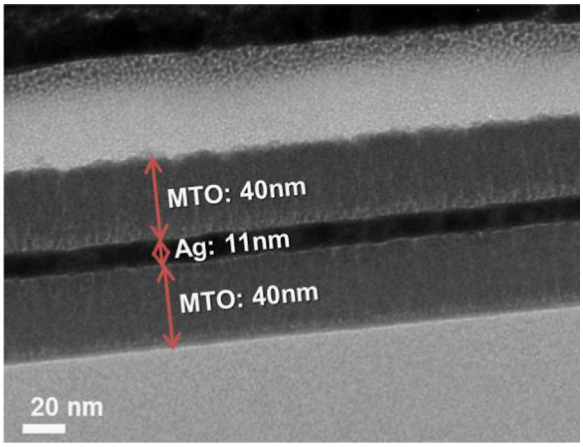

Fig. 5. Cross sectional TEM image of MTO/Ag/MTO multilayer electrode.

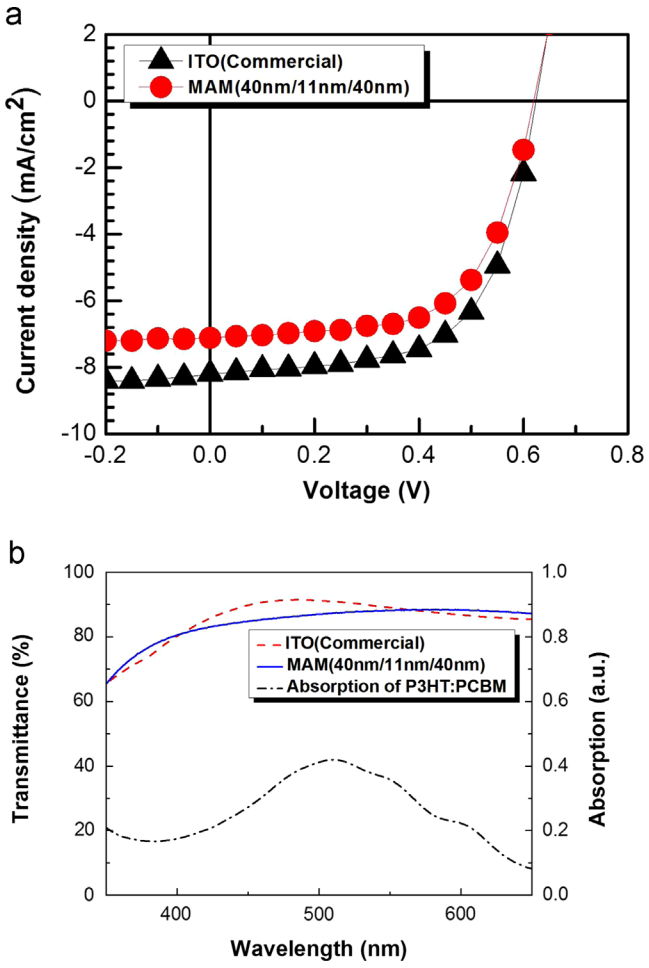

Fig. 6. (a) Current density–voltage (J–V) curve of the optimized MTO/Ag/MTO multilayer and ITO as a reference based on OPVs, (b) absorption of P3HT:PCBM active layer and transmittance of the optimized MTO/Ag/MTO multilayer and ITO as a reference.

optimized MTO (40 nm)/Ag (11 nm)/MTO (40 nm) multilayer electrode by TEM. It shows that each layer of the MTO/Ag/MTO multilayer electrode was uniformly deposited. The structural and optical properties of the MAM as grown and annealed using air at different temperatures (150–450 °C) was also studied (see Fig. S2 and S3, Supporting information). The highest transmittance and lowest surface resistance of the MAM films can be obtained through 250 °C annealing in air (see Table S1, Supporting information).

$$\frac{1}{R_S}=\frac{1}{R_{\text{Bottom-MTO}}}+\frac{1}{R_{\text{Middle-Ag}}}+\frac{1}{R_{\text{Top-MTO}}} \quad (2)$$

3.3. OPVs using MTO/Ag/MTO multilayer electrode

Conventional BHJ-OPVs were fabricated both on the optimized MTO/Ag/MTO electrode and on the commercial ITO electrode for comparison. Fig. 6(a) shows the current density–voltage (J–V) curve of BHJ-OPVs from the MTO/Ag/MTO multilayer electrode and the commercial ITO as a transparent electrode. Table 2 shows the comparison of OPV's performance on the MTO/Ag/MTO and the commercial ITO. The commercial ITO shows open circuit voltage (V_{OC}) of 0.62 V, short circuit current (J_{SC}) of 8.21 mA/cm^2, fill factor (FF) of 0.62 and power conversion efficiency (PCE) of 3.17%. Whereas, the MTO (40 nm)/Ag (11 nm)/MTO (40 nm) multilayer electrode shows a V_{OC} of 0.62 V, J_{SC} of 7.12 mA/cm^2, FF of 0.62 and PCE of 2.73%. As shown in Table 2, although these values were a little lower than that of commercial ITO and D(dielectric)/M/O electrodes [20,21], the efficiency was of slightly higher value [13–15,23] and similar value [22] than that of the BHJ-OPVs of published works (O/M/O). Lower PCE of the BHJ-OPVs adapting MTO/Ag/MTO multilayer compared to ITO can be explained from the short circuit current (J_{SC}) and work function. As shown in Table 2, V_{OC} and FF are the same except for J_{SC}. Short circuit current

Table 2
Comparison of OPVs performance of the optimized MTO/Ag/MTO multilayer, ITO and other published works.

Transparent electrode	V_{OC} (V)	J_{SC} (mA/cm^2)	FF	PCE (%)
ITO (Commercial)	0.62	8.21	0.62	3.17
MAM (40/11/40)	0.62	7.12	0.62	2.73
AZO/Ag/AZO (Ref. [13])	0.50	9.41	0.46	2.14
ZnO/Ag/ZnO (Ref. [14])	0.54	9.50	0.50	2.58
SnO_X/Ag/SnO_X (Ref. [15])	0.62	8.11	0.54	2.70
ZnS/Cu/WO_3 (Ref. [20])	0.60	8.1	0.70	3.40
ZnS/Ag/WO_3 (Ref. [21])	0.61	6.83	0.70	2.92
ZTO/Ag/ZTO (Ref. [22])	0.64	7.06	0.62	2.80
MoO_3/Au/MoO_3 (Ref. [23])	0.59	6.7	0.63	2.50

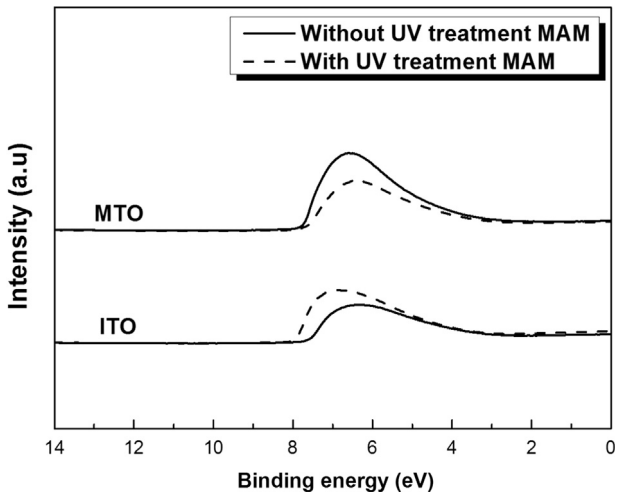

Fig. 7. UPS of optimized MTO/Ag/MTO multilayer and ITO with and without UV treatment.

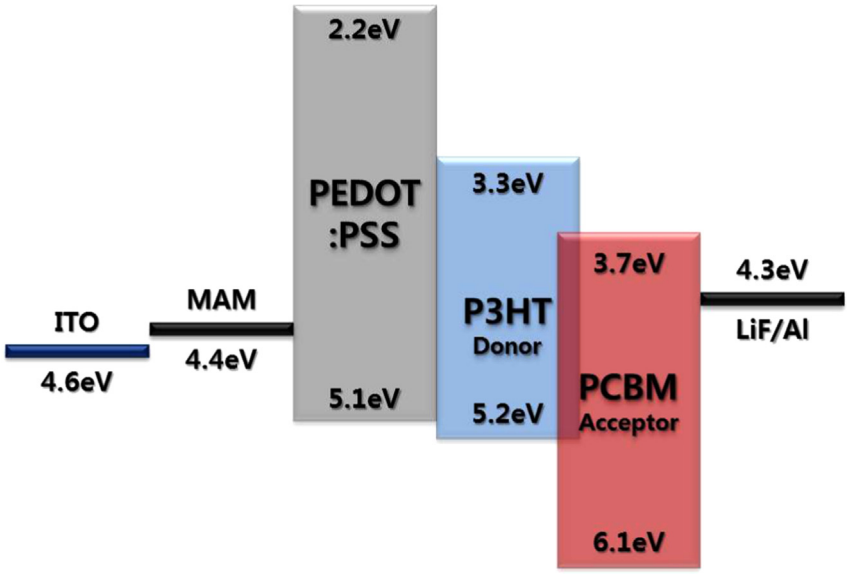

Fig. 8. Energy level diagram of BHJ-OPVs.

(J_{SC}) is defined by:

$$J_{SC} = \frac{\varepsilon_A \varepsilon_{ED} \varepsilon_{CT} \varepsilon_{CC}}{\text{Area}} \quad (3)$$

where ε_A is the light absorption efficiency, ε_{ED} is an exciton diffusion efficiency, ε_{CT} is a charge transfer efficiency, and ε_{CC} is a charge collection efficiency. In Eq. (3), ε_A of active layer is the most important factor which affects the efficiency of OPVs. In addition, if ε_A is increased, electrons and holes are easily excited. Thus the efficiency of OPVs will be increased. As shown in Fig. 6(b), the absorption of the P3HT:PCBM active layer mainly appeared at the wavelength range of 400–600 nm. However, the average transmittance at the wavelength of 400–600 nm of the MTO/Ag/MTO multilayer electrode was 86.3%. It was lower than that of the ITO electrode (88.7%). In general photons are easily transferred to the P3HT:PCBM active layer when transmittance is high. Hence, ε_A of active layer of OPVs using the MTO/Ag/MTO multilayer electrode is lower than that of the ITO electrode. As shown in Fig. 7, work functions of the MTO/Ag/MTO and ITO electrodes before UV treatment were 4.4 eV and 4.2 eV, respectively. After the UV treatment for control work function, they were modified 4.2 eV and 4.6 eV, respectively. Hence, as shown in Fig. 8, OPVs were manufacrured without UV treatment using the MTO/Ag/MTO multilayer electrode (4.4 eV). Consequently, the work function of the MTO/Ag/MTO after UV treatment was lower than that of ITO. When the MTO/Ag/MTO was adapted as anode, hole formed from active layer was expected for easy recombination before transfer from HTL to anode compared to the ITO electrode. Therefore, the PCE was decreased.

4. Conclusion

In single MTO thin film, electrical and optical properties were influenced by working pressure and oxygen partial pressure. The best performance was measured at the thickness of the Ag thin film of 11 nm in the MTO/Ag/MTO structure. The highest transmittance (T_{ave} (380–770 nm) were of 87.19% and surface resistance of 9.06 Ω/sq. of the MAM films were obtained through 250 °C annealing in air. BHJ-OPVs using the MTO/Ag/MTO multilayer electrode show PCE of 2.73%, but it is lower value than that for ITO of 3.17%. The reason for the low value can be explained by lower work function and lower transmittance at wavelengths of 400–600 nm compared to the ITO electrode. However, work function (4.4 eV) of the MTO/Ag/MTO multilayer electrode without UV treatment is expected to enhance performance at inverted OPVs structure.

Acknowledgments

This work was partially supported by the Converging Research Center Program through the Ministry of Science, ICT and Future Planning, Korea (2013K000199) and KIST program (2E24871).

Appendix A. Supporting information

Supplementary data associated with this article can be found in the online version at http://dx.doi.org/10.1016/j.solmat.2014.08.025.

References

[1] J.-A. Jeong, H.-K. Kim, Al_2O_3/Ag/Al_2O_3 multilayer thin film passivation prepared by plasma damage-free linear facing target sputtering for organic light emitting diodes, Thin Solid Films 547 (2013) 63–67.
[2] C. Guillén, J. Herrero, TCO/metal/TCO structures for energy and flexible electronics, Thin Solid Films 520 (2011) 1–17.
[3] Y.-S. Park, K.-H. Choi, H.-K. Kim, J.-W. Kang, Stacking sequence effect on the electrical and optical properties of multistacked flexible IZO/Ag/IZO electrodes, Electrochem. Solid-State Lett. 13 (2010) 39–42.
[4] G.B. Murdoch, S. Hinds, E.H. Sargent, S.W. Tsang, L. Mordoukhovski, Z.H. Lu, Aluminum doped zinc oxide for organic photovoltaics, Appl. Phys. Lett. 94 (2009) 213301.
[5] J.C. Wang, X.C. Ren, S.Q. Shi, C.W. Leung, Paddy K.L. Chan, Charge accumulation induced S-shape *J–V* curves in bilayer heterojunction organic solar cells, Org. Electron. 12 (2011) 880–885.
[6] M.S. Ryu, J. Jang, Effect of solution processed graphene oxide-nickel oxide bilayer on cell performance of bulk-heterojunction organic photovoltaic, Sol. Energy Mater. Sol. Cells 95 (2011) 2893–2896.
[7] Soniya D Yambemn, K.-S. Liao, SeamusA. Curran, Flexible Ag electrode for use in organic photovoltaics, Sol. Energy Mater. Sol. Cells 95 (2011) 3060–3064.
[8] Radhouane Bel Hadj Tahar, Takayuki Ban, Yutaka Ohya, Yasutaka Takahashi, Tin doped indium oxide thin films: electrical properties, J. Appl. Phys. 83 (1998) 2631.
[9] J.-W. Lim, S.-I. Oh, K.T. Eun, S.-H. Choa, H.-W. Koo, T.-W. Kim, H.-K. Kim, Mechanical flexibility of ZnSnO/Ag/ZnSnO films grown by roll-to-roll sputtering for flexible organic photovoltaics, Jpn. J. Appl. Phys. 51 (2012) 115801.
[10] Christopher J.M. Emmott, Antonio Urbina, Jenny Nelson, Environmental and economic assessment of ITO-free electrodes for organic solar cells, Sol. Energy Mater. Sol 97 (2012) 14–21.
[11] H. Kim, C.M. Gilmore, A. Piqué, J.S. Horwitz, H. Mattoussi, H. Murata, Z.H. Kafafi, D.B. Chrisey, Electrical, optical, and structural properties of

indium–tin oxide thin films for organic light-emitting devices, J. Appl. Phys. 86 (1999) 6451.
[12] Y.-J. Shin, G.-E. Jang, Characteristics of indium-free ZTO/Ag/ZTO multilayer electrode grown on glass substrate at room temperature, J. Ceram. Process. Res. 13 (2012) 224–228.
[13] H.-K. Park, J.-W. Kang, S.-I. Na, D.-Y. Kim, H.-K. Kim, Characteristics of indium-free GZO/Ag/GZO and AZO/Ag/AZO multilayer electrode grown by dual target DC sputtering at room temperature for low-cost organic photovoltaics, Sol. Energy Mater. Sol. Cells 93 (2009) 1994–2002.
[14] Ahmad El Hajj, Sylvain Vedraine, Philippe Torchio, Bruno Lucas, Optimized ITO-free tri-layer electrode for organic solar cells, Org. Electron. 14 (2013) 1122–1129.
[15] J.-D. Yang, S.-H. Cho, T.-W. Hong, D.I. Son, D.-H. Park, K.-H. Yoo, W.-K. Choi, Organic photovoltaic cells fabricated on SnO_X/Ag/SnO_X multilayer transparent conducting electrode, Thin Solid Films 520 (2012) 6215–6220.
[16] R.D. Shannon, Revised effective ionic radii and systematic studies of interatomic distances in halides and chalcogenides, Acta Cryst A32 (1976) 751–767.
[17] C.-H. Lee, B.-A. Nam, W.-K. Choi, J.-K. Lee, D.-J. Choi, Y.-J. Oh, Mn:SnO_2 ceramics as p-type oxide semiconductor, Mater. Lett. 65 (2011) 722–725.
[18] G. Haacke, New figure of merit for transparent conductors, J. Appl. Phys. 47 (1976) 4086.
[19] Y.-Y. Choi, K.-H. Choi, H.S. Lee, H.S. Lee, J.-W. Kang, H.-K. Kim, Nano-sized Ag-inserted amorphous $ZnSnO_3$ multilayer electrodes for cost-efficient inverted organic solar cells, Sol. Energy Mater. Sol. Cells 95 (2011) 1615–1623.
[20] S.Y. Lim, D.G. Han, H.Y. Kim, S.H. Lee, S.H. Yoo, Cu-based multilayer transparent electrodes: a low-cost alternative to ITO electrodes in organic solar cells, Sol. Energy Mater. Sol. Cells 101 (2012) 170–175.
[21] S.C. Han, S.Y. Lee, H.Y. Kim, H. Cho, S.H. Yoo, Versatile multilayer transparent electrodes for ITO-free and flexible organic solar cells, IEEE J. Sel. Top. Quant. Electron. 16 (2010) 1656–1664.
[22] S.-H. Cho, R. Pandey, C.-H. Wie, Y.J. Lee, J.-W. Lim, D.-H. Park, J.-S. Seok, Y.-H. Jang, K.-K. Kim, D.K. Hwang, D.-J. Byun, W.-K. Choi, Highly transparent ZTO/Ag/ZTO multilayer electrode deposited by inline sputtering process for organic photovoltaic cells, Phys. Status Solidi A (2014) 1–8. http://dx.doi.org/10.1002/pssa.201330594.
[23] W. Cao, Y. Zheng, Z. Li, E. Wrzesniewski, W.T. Hammond, J.G. Xue, Flexible organic solar cells using an oxide/metal/oxide trilayer as transparent electrode, Org. Electron. 13 (2012) 2221–2228.